

# Synthesis, characterization, and biological evaluation of new spebrutinib analogues: potential candidates with enhanced activity and reduced toxicity profiles

Zaid M Jaber Al-Obaidi <sup>Corresp., 1</sup>, Omar F Abdul-Rasheed <sup>2</sup>, Monther F Mahdi <sup>3</sup>, Ayad M R Raauf <sup>4</sup>

<sup>1</sup> Department of Pharmaceutical Chemistry, College of Pharmacy, University of Kerbala, Karbala, Karbala, Iraq

<sup>2</sup> Department of Chemistry and Biochemistry, College of Medicine, Al Nahrain University, Baghdad, Baghdad, Iraq

<sup>3</sup> Department of Pharmaceutical Chemistry, Ashur University College, Baghdad, Baghdad, Iraq

<sup>4</sup> Department of Pharmaceutical Chemistry, University of Mustansiriyyah, Baghdad, Baghdad, Iraq

Corresponding Author: Zaid M Jaber Al-Obaidi  
Email address: zaid.alobaidi@uokerbala.edu.iq

**Background:** Cancer is regarded as an undoubtable major concern for both researchers and the general public because of its high mortality rates. While breast cancer has the highest incidence of malignancy globally, colon cancer also has high morbidity and mortality rates. Currently, researchers are working on designing, synthesizing, and biologically investigating the effects of some potential anticancer candidates.

**Methods:** The authors successfully synthesized and characterized two potential spebrutinib analogues. These analogues were evaluated with the employment of MCF-7, HCT116, and MDCK cell lines.

**Results:** With respect to the spebrutinib standard, one of these analogues had superior activity against the MCF-7 cell line (IC<sub>50</sub>; 10.744 µg/mL against 13.566 µg/mL for spebrutinib) and an enhanced toxicity profile on the MDCK cell line (IC<sub>50</sub>; 8.653 mg/mL against 4.011 mg/mL for spebrutinib).

# **Synthesis, characterization, and biological evaluation of new spebrutinib analogues: potential candidates with enhanced activity and reduced toxicity profiles**

Zaid M. Jaber Al-Obaidi<sup>1</sup>, Omar F. Abdul- Rasheed<sup>2</sup>, Monther F. Mahdi<sup>3</sup>, Ayad M.R. Raauf<sup>4</sup>

<sup>1</sup> Department of Pharmaceutical Chemistry, College of Pharmacy, University of Kerbala, Karbala, Iraq.

<sup>2</sup> Department of Chemistry and Biochemistry, College of Medicine, Al- Nahrain University, Baghdad, Iraq.

<sup>3</sup> Department of Pharmaceutical Chemistry, Ashur University College, Baghdad, Iraq.

<sup>4</sup> Department of Pharmaceutical Chemistry, College of Pharmacy, Mustansiriyah University, Baghdad, Iraq.

Corresponding Author:

Zaid Al-Obaidi<sup>1</sup>

Karbala, Iraq

Email address: zaid.alobaidi@uokerbala.edu.iq

## **Abstract**

**Background:** Cancer is regarded as an undoubtable major concern for both researchers and the general public because of its high mortality rates. While breast cancer has the highest incidence of malignancy globally, colon cancer also has high morbidity and mortality rates. Currently, researchers are working on designing, synthesizing, and biologically investigating the effects of some potential anticancer candidates.

**Methods:** The authors successfully synthesized and characterized two potential spebrutinib analogues. These analogues were evaluated with the employment of MCF-7, HCT116, and MDCK cell lines.

**Results:** With respect to the spebrutinib standard, one of these analogues had superior activity against the MCF-7 cell line (IC<sub>50</sub>; 10.744 µg/mL against 13.566 µg/mL for spebrutinib) and an enhanced toxicity profile on the MDCK cell line (IC<sub>50</sub>; 8.653 mg/mL against 4.011 mg/mL for spebrutinib).

## **Introduction**

Cancer is the second leading cause of deaths worldwide [1] and is thus a major concern for researchers. Although death rates from communicable diseases have improved worldwide as a result of medical improvements, cancer-related mortality has increased by almost 40% in the past 40 years. In the next 15 years, a further 60% rise is expected, with 13 million people estimated to die of cancer in 2030 [2].

Breast cancer has the highest global incidence of malignancy among women, representing 25% of all cancers. A higher mortality rate has been shown to be even higher among women, especially in low-income countries [3]. In a published study, the incidence of breast cancer in Iraqi women was found to represent 33.8% of all cancers registered in females aged  $\geq 15$  years in Iraq during 2000-2009, with a total of 23,792 confirmed cases [4].

Colon cancer, diverted malignancies of the gastrointestinal tract, also has high global morbidity and mortality rates [5,6]. This is associated with timely progressive incidence [7]. The United States and Europe are considered as the regions with highest incidence [8]. China comes in third place in colon malignant tumour incidence [9].

Therefore, there is a compelling need to develop new drugs to treat this life-threatening disease. Conventional chemotherapy is associated with several side effects [10]. In recent years, the development and use of small molecules such as tyrosine kinase inhibitors (Imatinib, Spebrutinib, Gefitinib, Sunitinib, semaxinib etc.) in the treatment of cancer has helped scientists understand the molecular mechanisms of this disease [11]. Targeting enzymes involved in the signal transduction pathways of protein kinases that regulate cellular growth and multiplication is one of the approaches in developing new anticancer drugs [12,13].

Scientists have also recognized tyrosine kinases as potential targets to suppress or even cure breast cancers [14]. Consequently, many tyrosine kinase inhibitors (TKI) have been developed and tested [15-17], but the off-target serious side effects of these TKIs are a major obstacle [18-21].

For some prestigious journal publishers, the biological investigation of newly synthesized potential anticancer candidates is necessary [22]. In this work, the authors aimed to synthesize, characterize, and biologically evaluate new TKIs that show superior activity and reduced toxicity.

## Materials & Methods

### 2.1 Materials:

The materials used in this work are shown in Table 1.

### 2.2 Cell lines

The following types of cell lines were used in this study:

1. MCF-7 Breast cancer
2. HCT116 colorectal cancer cells
3. MDCK kidney normal cells.

Cell lines were kindly contributed from the international cell line collection of Dr. Hamid N. Obied (M.B.CH.B., MSc, PhD Pharmacology, Lecturer and researcher in anticancer at the Department of Clinical Pharmacology, College of Medicine, University of Babylon, and the head of the cancer cell research unit at the Al-Fadhil Foundation for educational services, training and development – branch of Babylon).

## 2.3 Instruments

The instruments used in this work are listed in Table 2.

## 2.4 Methods:

### 2.5 Chemical synthesis:

The overall chemical syntheses are revealed in scheme (1).

The following chemical methods were used for the spebrutinib analogue preparations [15]:

#### 2.5.1 Synthesis of compound (2a) N-(3-((5-fluoro-2-((4-(2-methoxyethoxy)phenyl)amino)pyrimidin-4-yl)amino)phenyl)benzamide.

1. Benzoyl chloride (309 mg, 2.2 mmol) was added to a stirred solution of compound (1) (665 mg, 1.8 mmol) and potassium carbonate (1.24 g, 9 mmol) in THF (12 mL) at 0°C, and the reaction mixture was stirred at 0°C for 45 min.

2. The reaction mixture was added drop-wise to a cold solution of 10% NaHCO<sub>3</sub> (12 mL) while being stirred, and was stirred at the same temperature (0°C) for 30 min.

3. A solid precipitate was isolated by filtration and washed with cold water and hexane, and then was dissolved in a mixture of methanol/dichloromethane (50:50, 10 mL) and was concentrated under reduced pressure.

4. The residue obtained was suspended in cold water (20 mL), Et<sub>3</sub>N was added to it, and then it was extracted with ethyl acetate (2 x 20 mL).

5. The combined ethyl acetate extract was washed with water (10 mL) and concentrated under reduced pressure in a desiccator to get 2-a (0.761 mg, 89%).

#### 2.5.2 Synthesis of compound (2-b) N-(3-((5-fluoro-2-((4-(2-methoxyethoxy)phenyl)amino)pyrimidin-4-yl)amino)phenyl)pivalamide.

1. Trimethylacetyl chloride (266 mg, 2.2 mmol) was added to a stirred solution of compound (1) (665 mg, 1.8 mmol) and potassium carbonate (1.24 g, 9 mmol) in THF (12 mL) at 0°C, and the reaction mixture was then stirred at 0°C for 45 min.

2. The reaction mixture was added drop-wise to a cold solution of 10% NaHCO<sub>3</sub> (12 mL) being stirred, and was stirred at the same temperature (0°C) for 30 min.

3. A solid precipitate was isolated by filtration and washed with cold water and hexane, was dissolved in a mixture of methanol/dichloromethane (50:50, 10 mL) and was concentrated under reduced pressure.

4. The residue obtained was suspended in cold water (20 mL), Et<sub>3</sub>N was added to it, and then it was extracted with ethyl acetate (2 x 20 mL).

5. The combined ethyl acetate extract was washed with water (10 mL) and concentrated under reduced pressure in a desiccator to get 2b (0.705 mg, 86%).

## 2.6 Cell line preparation:

The cell lines were cultured in medium 1640 (RPMI-1640, Gibco-BRL), with 10% heat-inactivated fetal bovine serum (FBS) (Gibco). Cell lines were allocated in Celltreat® 96 well cell culture plates and incubated to grow at 37°C. The time of cell culture was optimized to 24 hours (from 72 hours originally) and the steps involved in the cell line part of this work are listed below:

## 2.7 MTT stock solution preparation:

25-mg was accurately weighed and transferred into a suitable flask. Then, 5-ml of DMSO was added and the MTT was completely dissolved. The 5-ml of 5mg/ml was filtered into a 12.mL centrifuge tube with 0.22µm sterile filters, and the tube was foiled with aluminium sheet as the MTT solution is light sensitive. This solution was kept in the fridge during the preparation of the working solution.

## 2.8 MTT working solution preparation:

According to the protocols, the working concentration of MTT is 0.5mg/ml. This is 10% v/v of the stock solution. For a final volume of 12 ml of cell-medium with 10% MTT, the following dilutions were performed. 10.600 ml of cell medium was accurately measured and allocated into a suitable flask. Then 2.400 ml of MTT stock solution was added to the medium and adequately homogenized. The cell-medium with 10% MTT was ready to be utilized for cell-lines and an incubation period of 3 hrs.

## 2.9 Preparation of working concentrations from each test chemical for the cell-lines:

A suitable amount of each chemical was dissolved in DMSO to get a stock solution with a concentration of 5mg/ml for each chemical and standard. After several cell line trials, the concentration was optimized for 50µg/ml as the higher concentration from which a serial dilution was performed. For each standard and synthesized chemical, 990-µl of the medium was accurately measured and 10-µl from the 5mg/ml was added and homogenized to get a final concentration of 50 µg/ml and a final concentration of 1% for the DMSO. Serial dilution was performed for each to get the following concentrations: 50, 25, 12.5, 6.25, 3.125, and 1.5625 µg/ml.

## 2.10 Stock solution preparation:

An accurately weighed amount of each synthesized chemical compound was dissolved in pure DMSO to get a concentration of 5mg/mL. After complete dissolution, the solutions were filtered through a 0.2 µm sterile filter. 10 µL of the above filtrate was further diluted with 990 µL of RPMI-1640 medium to get a final concentration of 50 µg/mL. A serial dilution was prepared from the above concentration to get 50, 25, 12.5, 6.25, and 3.125 µg/mL.

## 2.11 Application of the chemicals on the cell-lines:

The above serial dilution solutions were added in 200 µl portions for each well in triplicates and incubated for 24 hrs. After the incubation period, the plates were visualized with an inverted

microscope and screen shots were captured for each well. The media was replaced with 10% MTT media and incubated for 3 hours. After the 3 hours of incubation, the media was removed, and the wells were washed with phosphate buffer saline (PBS). Finally, a 200.μl portion of DMSO was added into each well and left for 30 minutes and was read with a plate reader at 630 nm.

## Results and Discussion

### 3.1 Results of chemical synthesis:

The data supplied in Table 3 are valuable. The observed melting points were observed with a Differential Scanning Calorimeter (DSC), a very sensitive instrument from Shimadzu that provides the melting point to two decimal places, a task that is apparently impossible for the traditional capillary apparatus. In the DSC chart, the temperature is raised until the chemical compound reaches its melting point ( $T_m$ ). The chart will spike at that temperature, as the melting process causes an endothermic change that appears as a peak in the DSC curve. The DSC is considered a very sensitive technique to record characteristic melting points for various analytes, due to its capability to record enthalpies and transition temperatures with noticeable sensitivity [23]. In this study, the melting points were recorded for spebrutinib and the synthesized compounds.

The estimated log P (Octanol-water partition coefficient) parameters, hydrogen bond donors, and hydrogen bond acceptors comply well with Lipinski's rule of five. In 1997, Christopher A. Lipinski and his team tested many drug molecules and concluded that a compound is more likely to be orally active if it does not breach more than one of the following rules [24-28]:

1. Hydrogen bond donors < 5 (the sum of the N-H and O-H bonds).
2. Hydrogen bond acceptors < 10 (the sum of the N and O atoms).
3. A molecular mass no greater than 500 Daltons.
4. A log P no greater than 5.

However, rotatable bond count is another issue that correlates with the oral absorption feature of drugs. To have good oral bioavailability, the drug has to have no more than 10 rotatable bonds. This feature is achieved with compound 2a. In the same context, the drug likeliness is close if the topological polar surface area is equal to or less than 140 Å<sup>2</sup>, which has been observed for all the synthesized compounds [29].

The tPSA is the summation of the total polar atoms on the surface of a molecule, and these atoms basically are comprised of oxygen and nitrogen along with the attached hydrogens. tPSA is a widely utilized tool in medicinal chemistry to judge whether a drug is capable of permeating into cells. To permeate into enterocytes and become orally bioavailable, the tPSA of a molecule has to be lower than 140 square angstroms, and a tPSA less than 90 square angstroms confirms the molecules are able to penetrate the blood-brain barrier and become bioavailable to the CNS [30-32].

In chemistry, the amount of product obtained in a chemical reaction divided by the amount calculated for a theoretical yield is known as the percent yield, which is a measure of the reaction efficiency. Yields less than 40% are considered poor, more than 50% are considered fair, greater than 70% are considered good, greater than 80% are very good, greater than 90% are excellent, and yields near 100% are known as quantitative yields [33,34]. Accordingly, the percent yields of the chemical syntheses in this work are considered very good.

Three spebrutinib analogues were successfully synthesized. Thereafter, the selected chemical and physical parameters of the synthesized compounds are tabulated in Table 3 and Table 4:

### 3.2 Results of characterization of the synthesized compounds:

#### 3.2.1 FT-IR Characterization:

Infrared spectroscopy is considered a fast, robust, non-destructive tool and is utilized frequently in drug analysis and characterization [35]. The carbonyl functional group is very characteristic of chemical compounds when employing FT-IR instrumentation [36]. In this work, FT-IR was primarily utilized to identify and confirm the structures of the synthesized compounds based on the appearance and disappearance of the characteristic bands in the observed spectra. The appearance of the amide carbonyl band was characteristic of all shown spectra.

3.2.1.1 FT-IR Characterization of compound 2a  
3272 cm<sup>-1</sup> (N-H stretch of amide), 1649 cm<sup>-1</sup> (C=O stretch of amide), 1492 cm<sup>-1</sup> (C-C stretch of aromatic), 1437 cm<sup>-1</sup> (C-C stretch of aromatic (in-ring)).

3.2.1.2 FT-IR Characterization of compound 2b  
3432 cm<sup>-1</sup> (N-H stretch of amide), 3364 cm<sup>-1</sup> and 3207 cm<sup>-1</sup> (N-H stretch of 2° amines), 1660 cm<sup>-1</sup> (C=O stretch of amide), 1424 cm<sup>-1</sup> (C-C stretch of aromatic (in-ring)).

3.2.2 Elemental Microanalysis (CHN):  
Elemental microanalysis is considered a fundamental tool for chemical compound identification. It measures the elemental carbon, hydrogen, and nitrogen (CHN) contents of a chemical compound using an elemental analyzer [37]. High-accuracy CHN analyzers have been globally utilized for chemical compound identification, and in general, an error no greater than 0.4% is required for these types of analyses [38]. In this study, all the synthesized compounds had errors less than 0.4% (0.21%-0.37%), which indicates a high accuracy and low content of impurities. Elemental microanalyses were performed for the spebrutinib and the synthesized compounds, and the results are tabulated in Table 5.

3.2.3 <sup>1</sup>H NMR Characterization:  
3.2.3.1 <sup>1</sup>H NMR Characterization of compound 2a and their interpretations are shown in Table 6.  
3.2.3.2 <sup>1</sup>H NMR Characterization of compound 2b and their interpretations are shown in Table 7.  
Results of the biological effect of the synthesized compounds on cancerous and normal cell-lines:

3.3 Effect on HCT116 colorectal cancer cell-line:

3.3.1 The effect of Spebrutinib is shown in Figure 1.

3.3.2 The effect of compound 2a is shown in Figure 2.

3.3.3 The effect of compound 2b is shown in Figure 3.

3.4 Effect on MCF-7 breast cancer cell-line:

3.4.1 The effect on the MCF-7 breast cancer cell-line is shown in Figure 4.

3.4.2 The effect of compound 2a is shown in Figure 5.

3.4.3 The effect of compound 2b is shown in Figure 6.

3.5 Effect on MDCK kidney normal cell-line:

The ex vivo toxicity of the synthesized spebrutinib analogues were evaluated by applying these synthesized chemicals on the Madin-Darby Canine Kidney (MDCK) epithelial cell line (non-cancerous, normal kidney cells). These cells were derived by S. H. Madin and N. B. Darby from the kidney tissue of an adult female cocker spaniel.

3.5.1 The effect of Spebrutinib is shown in Figure 7.

3.5.2 The effect of compound 2a is shown in Figure 8.

3.5.3 The effect of compound 2b is shown in Figure 9.

The IC<sub>50</sub> for the synthesized compounds and the spebrutinib standard for the HCT116, MCF-7, and the MDCK cell lines are shown in Table 8.

Results of the biological effect of the synthesized compounds on the cancerous and normal cell-lines:

The time of incubation was optimized to 48 hours instead of 72 hours, and eventually an incubation period of 24 hours was selected. The concentrations of the synthesized chemicals that were applied to the cells were optimized, starting with the highest concentration of 1 mg/L and reaching the optimized high concentration of 50 µg/mL.

Thereafter, the serial dilution performed from 50 µg/mL was mathematically accepted to give good representative curves. The sketched curves possessed good correlation coefficients. Furthermore, the half maximal inhibitory concentration (IC<sub>50</sub>) values were mostly in the middle of the curves to exclude any proposed drift in the curves if any existed. The IC<sub>50</sub> is a measure of the effectiveness of the synthesized chemical compound in inhibiting cell growth.

The cell lines were meaningfully chosen and accurately selected. Colorectal cancer is classified as the third most common cancer, excluding skin cancers, in occurrence in the US for both sexes. The American Cancer Society has proposed the number of colorectal cancer cases as 44,180 new cases of rectal cancer and 101,420 new cases of colon cancer in 2019 [39]. Excluding skin cancers, breast cancer is classified as the highest occurring cancer in the US for women. The American Cancer Society has estimated the number of breast cancer cases in 2019 as 268,600 new cases of invasive breast cancer and 62,930 new cases of non-invasive breast cancer. [40].

To evaluate the selectivity of the newly synthesized compounds toward the cancer cells, it is essential to test their toxicity on normal (non-cancerous) cells [41,43]. A large number of authors have utilized the MDCK cell line for cell viability studies [44-52]. Because of this fact, and their availability, the MDCK cell lines were selected.

Table 8 shows the net results of this work, revealing the biological effects of the chemically synthesized compounds on cancerous and normal cells. This brief comparison gives valuable information. To critically analyse the observed data, it will be categorized below for each compound and then for each cell :

1. The spebrutinib standard shows close values of IC<sub>50</sub> for both HCT116 and MCF-7 cell lines with priority for the HCT116 cells. In the same context of spebrutinib, the IC<sub>50</sub> for MDCK cells shows approximately 300-fold the concentration required for the activity against both HCT116 and MCF-7 cell lines. This reveals a much greater selectivity toward cancerous cells than toward the normal non-cancerous cells.

2. For compound 2a, the IC<sub>50</sub> value for the HCT116 cells is three-fold its value for MCF-7 cells. In other words, compound 2a has superior activity for MCF-7 cells than for the HCT116 cells. Moreover, the IC<sub>50</sub> of compound 2a for MDCK shows approximately 250-fold and 800-fold of the concentration required for activity against the HCT116 and MCF-7 cell lines, respectively. This indicates an excellent selectivity toward the cancerous cells, with better selectivity toward the MCF-7 cell line.

3. For compound 2b, the IC<sub>50</sub> value for the HCT116 cells is 1.3-fold its value for MCF-7 cells. Accordingly, compound 2b has better activity for MCF-7 cells than for the HCT116 cells. Moreover, the IC<sub>50</sub> of compound 2b for MDCK shows approximately 67-fold and 89-fold of the concentration required for activity against the HCT116 and MCF-7 cell lines, respectively. This indicates an acceptable selectivity margin toward the cancerous cells, with better selectivity toward the MCF-7 cell line.

According to the European Medicines Agency (EMA) (with respect to the “Nonclinical Evaluation for Anticancer Pharmaceuticals”), “a common approach for many small molecules is to set a start dose at 1/10 the Severely Toxic Dose in 10% of the animals (STD 10) in rodents [30]. If the non-rodent is the most appropriate species, then 1/6 the Highest Non-Severely Toxic Dose (HNSTD) is considered an appropriate starting dose. The HNSTD is defined as the highest dose level that

does not produce evidence of lethality, life-threatening toxicities or irreversible findings” [53]. In all the previously discussed findings, the proposed therapeutic doses are much lower than the “one-tenth” portion of the STD 10. Accordingly, the therapeutic doses can be reduced to be equal or below the micromolar concentrations recommended by many researches [54,56]

4. For the HCT116 cell line, the IC<sub>50</sub> for the spebrutinib standard has the lowest value, followed by compound 2b and lastly compound 2a. Compound 2b has twice the IC<sub>50</sub> value when compared to the spebrutinib standard, and compound 2a has trice the IC<sub>50</sub> value for the standard.

5. The MCF-7 cell line has the most interesting findings. Compound 2a has the lowest IC<sub>50</sub> value, which indicates better cytotoxic activity than the spebrutinib standard. Spebrutinib has the middle value for IC<sub>50</sub> (1.25 times of that of compound 2a). Finally, compound 2b has the highest IC<sub>50</sub> value.

6. For the MDCK cell line, the IC<sub>50</sub> values reveal valuable information. For example, compound 2b has the lowest IC<sub>50</sub> value, which means it is the most toxic in respect to compounds 2a and standard. On the other hand, the IC<sub>50</sub> for compound 2a has approximately twice the IC<sub>50</sub> value of that of the spebrutinib standard. To summarize, compound 2a has better activity and lower toxicity than the spebrutinib standard.

## Conclusions

In this work, the authors conclude that the two new spebrutinib analogues were successfully synthesized and characterized, and the synthesized compounds were found to have biological activity. For the biological effects against breast cancer cell lines, compound 2b has approximately 1.4-times the IC<sub>50</sub> value of that of spebrutinib. Compound 2a has the lowest IC<sub>50</sub> value, approximately 0.8-times that of spebrutinib. This indicates better cytotoxic activity than the spebrutinib standard. Furthermore, compound 2a has a better toxicity profile (IC<sub>50</sub> 8.633 mg/mL) regarding the normal kidney cell line in respect to spebrutinib (IC<sub>50</sub> 4.011 mg/mL).

## Acknowledgements

The authors would like to acknowledge the laboratory and logistical support supplied by the College of Pharmacy, University of Kerbala, the College of Pharmacy, Mustansiriyah University, and the College of Medicine, University of Babylon.

## References

1. Papac RJ. (2001). Origins of cancer therapy. The Yale journal of biology and medicine. 74 (6):3916.
2. Kuipers EJ, Rösch T & Bretthauer M. (2013). Colorectal cancer screening — optimizing current strategies and new directions. Nat. Rev. Clin. Oncol. 10, 130 –142.
3. Nada A.S. Alwan (2016), Breast Cancer Among Iraqi Women: Preliminary Findings From a Regional Comparative Breast Cancer Research, Journal of Global Oncology.

4. Muzahem Mohammed Yahya AL-Hashimi\*, Xiang Jun Wang (2014). Breast Cancer in Iraq, Incidence Trends from 2000-2009, Asian Pacific Journal of Cancer Prevention.
5. Liu C, Huang Z, Jiang H, Shi F (2014) The sirtuin 3 expression profile is associated with pathological and clinical outcomes in colon cancer patients. Biomed Res Int 2014: 871263.
6. Kang M, Martin A (2017) Microbiome and colorectal cancer: Unraveling host- microbiota interactions in colitis-associated colorectal cancer development. Semin. Immunol 32: 3-13.
7. Liu X, Duan B, Dong Y, He C, Zhou H, et al. (2014) MicroRNA-139-3p indicates a poor prognosis of colon cancer. Int J Clin Exp Pathol 7: 8046-8052.
8. Hou Y, Liu YY, Zhao XK (2013) Expression of aldehyde dehydrogenase 1 in colon cancer. Asian Pac J Trop Med 6: 574-577.
9. Zhou E, Huang Q, Wang J, Fang C, Yang L, et al. (2015) Up-regulation of Tim-3 is associated with poor prognosis of patients with colon cancer. Int J Clin Exp Pathol 8: 8018-8027.
10. Zerhoef MJ, Rose MS, White M and Balneaves LG. (2008). Declining conventional cancer treatment and using complementary and alternative medicine: a problem or a challenge? Current Oncology. 15 (Suppl 2):s101.
11. Haddad JJ. (2012). The immunopharmacologic potential of Semaxanib and new generation directed therapeutic drugs: Receptor tyrosine kinase regulation with anti-tumorigenesis/angiogenesis properties. Saudi Pharmaceutical Journal. 20 (2):103-23.
12. Broekman F, Giovannetti E and Peters GJ. (2011). Tyrosine kinase inhibitors: Multi-targeted or single-targeted? World J Clin Oncol. 2 (2):80-93.
13. Wolle, P., et al. (2019). "Targeting the MKK7–JNK (Mitogen-Activated Protein Kinase Kinase 7–c-Jun N-Terminal Kinase) Pathway with Covalent Inhibitors." Journal of Medicinal Chemistry.
14. Burstein, H. J., et al. (2008). "Phase II study of sunitinib malate, an oral multitargeted tyrosine kinase inhibitor, in patients with metastatic breast cancer previously treated with an anthracycline and a taxane." Journal of Clinical Oncology 26(11): 1810-1816.
15. Bensinger, D., et al. (2019). "Virtual Screening Identifies Irreversible FMS-like Tyrosine Kinase 3 Inhibitors with Activity Toward Resistance-Confering Mutations." Journal of Medicinal Chemistry.
16. Popow, J., et al. (2019). "Highly Selective PTK2 Proteolysis Targeting Chimeras to Probe Focal Adhesion Kinase Scaffolding Functions." Journal of Medicinal Chemistry.
17. Simpson, G. L., et al. (2019). "Identification and Optimization of Novel Small c-Abl Kinase Activators Using Fragment and HTS Methodologies." Journal of Medicinal Chemistry 62(4): 2154-2171.
18. Steegmann, J. L., et al. (2012). "Off-target effects of BCR–ABL1 inhibitors and their potential long-term implications in patients with chronic myeloid leukemia." Leukemia & lymphoma 53(12): 2351-2361.

19. Yang, B. and T. Papoian (2012). "Tyrosine kinase inhibitor (TKI)-induced cardiotoxicity: approaches to narrow the gaps between preclinical safety evaluation and clinical outcome." *Journal of Applied Toxicology* 32(12): 945-951.
20. Force, T. and R. Kerkelä (2008). "Cardiotoxicity of the new cancer therapeutics—mechanisms of, and approaches to, the problem." *Drug discovery today* 13(17-18): 778-784.
21. Kerkela, R., et al. (2009). "Sunitinib-induced cardio-toxicity is mediated by off-target inhibition of AMP-activated protein kinase." *Clinical and translational science* 2(1): 15-25.
22. American Chemical Society, "Author Guide", 2018, [https://pubs.acs.org/paragonplus/submission/orlef7/orlef7\\_authguide.pdf](https://pubs.acs.org/paragonplus/submission/orlef7/orlef7_authguide.pdf); Accessed 28.02.2019.
23. Dean JA (1995). *The Analytical Chemistry Handbook*. New York: McGraw Hill, Inc. pp. 15.1–15.5. ISBN 0-07-016197-6.
24. Lipinski CA, Lombardo F, Dominy BW, Feeney PJ (March 2001). "Experimental and computational approaches to estimate solubility and permeability in drug discovery and development settings". *Adv. Drug Deliv. Rev.* 46 (1–3): 3–26. doi:10.1016/S0169-409X(00)00129-0. PMID 11259830.
25. Lipinski CA (December 2004). "Lead- and drug-like compounds: the rule-of-five revolution". *Drug Discovery Today: Technologies.* 1 (4): 337–341. doi:10.1016/j.ddtec.2004.11.007.
26. Oprea TI, Davis AM, Teague SJ, Leeson PD (2001). "Is there a difference between leads and drugs? A historical perspective". *J Chem Inf Comput Sci.* 41 (5): 1308–15. doi:10.1021/ci010366a. PMID 11604031.
27. Leeson PD, Springthorpe B (November 2007). "The influence of drug-like concepts on decision-making in medicinal chemistry". *Nat Rev Drug Discov.* 6 (11): 881–90. doi:10.1038/nrd2445. PMID 17971784.
28. Li, S. K., & Chantasart, D. (2018). Skin Permeation Enhancement in Aqueous Solution: Correlation with Equilibrium Enhancer Concentration and Octanol/water Partition Coefficient. *Journal of Pharmaceutical Sciences*.
29. Veber et al. *J. Med. Chem.* (2002) 45(12) pp. 2615-2623.
30. Pajouhesh H, Lenz GR (Oct 2005). "Medicinal Chemical Properties of Successful Central Nervous System Drugs". *NeuroRx.* 2 (4): 541–553. doi:10.1602/neurorx.2.4.541. PMC 1201314. PMID 16489364.
31. Hitchcock SA, Pennington LD (May 2006). "Structure - Brain Exposure Relationships". *J. Med. Chem.* 49 (26): 7559–7583.
32. Caron, G., & Ermondi, G. (2016). Molecular descriptors for polarity: the need for going beyond polar surface area. *Future Medicinal Chemistry*, 8(17), 2013–2016. doi:10.4155/fmc-2016-0165

33. Vogel, A. I.; Tatchell, A. R.; Furnis, B. S.; Hannaford, A. J.; Smith, P. W. G. (1996). Vogel's Textbook of Practical Organic Chemistry (5th ed.). Pearson. ISBN 978-0582462366.
34. MCAT Organic Chemistry Review (2019), Online + Book – Kaplan Test Prep.
35. Brielle, Esther S.; Arkin, Isaiah T. (2018). "Site-Specific Hydrogen Exchange in a Membrane Environment Analyzed by Infrared Spectroscopy". The Journal of Physical Chemistry Letters. 9 (14): 4059–4065.
36. Tan, M. J., Pan, H.-C., Tan, H. R., Chai, J. W., Lim, Q. F., Wong, T. I., ... Kong, K. V. (2018). Flexible Modulation of CO-Release Using Various Nuclearity of Metal Carbonyl Clusters on Graphene Oxide for Stroke Remediation. Advanced Healthcare Materials, 7(5), 1701113.
37. V. P. Fadeeva, V. D. Tikhova, and O. N. Nikulicheva, J. Anal. Chem., 2008, 63, 1094.
38. Royal Society of Chemistry, "Author Guidelines", 2018, [https://pubs.acs.org/paragonplus/submission/orlef7/orlef7\\_authguide.pdf](https://pubs.acs.org/paragonplus/submission/orlef7/orlef7_authguide.pdf); Accessed 11.02.2019.
39. The American Cancer Society, "Key Statistics for Colorectal Cancer", 2019, <https://www.cancer.org/cancer/colon-rectal-cancer/about/key-statistics.html>, Accessed 12.02.2019.
40. The American Cancer Society, "Current year estimates for breast cancer", 2019, <https://www.cancer.org/cancer/breast-cancer/about/how-common-is-breast-cancer.html>, Accessed 12.02.2019.
41. Jie Liu, Xiao-Hua Zou, Qian-Ling Zhang, Wen-Jie Mei, Jian-Zhong Liu, and Liang-Nian Ji, "Synthesis, Characterization and Antitumor Activity of a Series of Polypyridyl Complexes," Metal-Based Drugs, vol. 7, no. 6, pp. 343-348, 2000.
42. Hanelt, M., Gareis, M., & Kollarczik, B. (1994). Cytotoxicity of mycotoxins evaluated by the MTT-cell culture assay. Mycopathologia, 128(3), 167–174.
43. Kovačević, S. Z., Karadžić, M. Ž., Vukić, D. V., Vukić, V. R., Podunavac-Kuzmanović, S. O., Jevrić, L. R., & Ajduković, J. J. (2018). Toward steroidal anticancer drugs: Non-parametric and 3D-QSAR modeling of 17-picolyl and 17-picolinylidene androstanes with antiproliferative activity on breast adenocarcinoma cells. Journal of Molecular Graphics and Modelling.
44. Mazzawi, N., Kimmel, E., & Tsarfaty, I. (2019). The effect of low-intensity ultrasound and met signaling on cellular motility and morphology.
45. Applied Ac Tsai, C.-P., & Tsai, H.-J. (2018). Influenza B Viruses in Pigs, Taiwan. Influenza and Other Respiratory ousitics, 143, 1–6.
46. Alam, J., Jeon, S., & Choi, Y. (2019). Determination of Anti-aquaporin 5 Autoantibodies by Immunofluorescence Cytochemistry. Methods in Molecular Biology, 79–87.
47. Singh, G., Arora, A., Kalra, P., Maurya, I. K., Ruizc, C. E., Estebanc, M. A., ... Sehgal, R. (2019). A strategic approach to the synthesis of ferrocene appended chalcone linked

- triazole allied organosilatrane: Antibacterial, Antifungal, Antiparasitic and Antioxidant studies. *Bioorganic & Medicinal Chemistry*.
48. Jia, S.-F., Hao, X.-L., Wen, Y.-Z., & Zhang, A. Y. (2019). Synthesis, cytotoxicity, apoptosis and cell cycle arrest of a monoruthenium(II)-substituted Dawson polyoxotungstate. *Journal of Coordination Chemistry*, 1–9.
49. Xiong, W., Zhao, G. D., Yin, X., Linghu, K. G., Chu, J. M. T., Wong, G. T. C., Wang, Y. T. (2019). Brij-grafted-chitosan copolymers with function of P-glycoprotein modulation: Synthesis, characterization and in vitro investigations. *Carbohydrate Polymers*.
50. Yu, Y., Tazeem, T., Xu, Z., Du, L., Jin, M., Dong, C. Wu, S. W. (2018). Design and Synthesis of Heteroaromatic Based Benzenesulfonamide Derivatives as Potent Inhibitors of H5N1 Influenza A Virus. *MedChemComm*.
51. Dar'in, D., Zarubaev, V., Galochkina, A., Gureev, M., & Krasavin, M. (2019). Non-chelating p-phenylidene-linked bis-imidazoline analogs of known influenza virus endonuclease inhibitors: Synthesis and anti-influenza activity. *European Journal of Medicinal Chemistry*, 161, 526–532.
52. Li, H., Li, M., Xu, R., Wang, S., Zhang, Y., Zhang, L., Xiao, S. (2018). Synthesis, structure activity relationship and in vitro anti-influenza virus activity of novel polyphenol-pentacyclic triterpene conjugates. *European Journal of Medicinal Chemistry*.
53. The European Medicines Agency, "ICH S9 Nonclinical Evaluation for Anticancer Pharmaceuticals", 2019, [https://www.ema.europa.eu/documents/scientific-guideline/ich-s-9-nonclinical-evaluation-anticancer-pharmaceuticals-note-guidance-nonclinical-evaluation\\_en.pdf](https://www.ema.europa.eu/documents/scientific-guideline/ich-s-9-nonclinical-evaluation-anticancer-pharmaceuticals-note-guidance-nonclinical-evaluation_en.pdf), Accessed 13.02.2019.
54. A. H. Sheikh, A. Khalid, F. Khan, A. Begum, *ChemistrySelect* 2019, 4, 228.
55. Jiao, Y. H., et al. (2019). "Synthesis of a novel p-hydroxycinnamic amide with anticancer capability and its interaction with human serum albumin." *Exp Ther Med* 17(2): 1321-1329.
56. Serhii Holota, Anna Kryshchishyn, Halyna Derkach, Yaroslava Trufin, Inna Demchuk, Andrzej Gzella, Philippe Grellier, Roman Lesyk, Synthesis of 5-enamine-4-thiazolidinone derivatives with trypanocidal and anticancer activity, *Bioorganic Chemistry*, Volume 86, 2019, Pages 126-136, ISSN 0045-2068.

# **Table 1**(on next page)

Utilized materials with their manufacturers and countries of origin.

**1 Table (1): Utilized materials with their manufacturers and countries of origin.**

#	Material	Manufacturer	Country
1	Spebrutinib AVL-292 (99.48%)	BLDpharm	CHINA
2	N4-(3-Aminophenyl)-5-fluoro-N2-(4-(2-methoxyethoxy)phenyl)pyrimidine-2,4-diamine (98%)	BLDpharm	CHINA
3	Tetrahydrofuran A.R. (99%)	SCR	CHINA
	Potassium carbonate A.R. (99%)	SCR	CHINA
4	Tetramethylacetyl chloride (99%)	Sigma-Aldrich	USA
5	Benzoyl chloride A.R. (99.5%)	CDH	INDIA
6	n-Hexane (95%)	GCC	UK
7	Dichloromethane HPLC-grade (99.8%)	GCC	UK
8	Sodium hydrogen carbonate, A.R. (99.5%)	HIMEDIA	INDIA
9	Methanol absolute HPLC-grade	Biosolve Chimie SARL	FRANCE
10	Dimethyl sulphoxide (99%)	CDH	INDIA
11	Cellulose acetate membrane filter pore size 0.2 µm diameter 25 mm.	chm	SPAIN
12	MTT (3-[4,5-dimethylthiazol-2-yl]-2,5-diphenyl tetrazolium bromide)	Roth	GERMANY
13	Celltreat® 96 Well Cell Culture Plates	CELLTREAT Scientific Products	USA

2

## Table 2 (on next page)

Employed instruments with their manufacturers and countries of origin.

1

2 **Table (2): Employed instruments with their manufacturers and countries of origin.**

#	Instrument	Manufacturer	Country
1	4-digit balance	Sartorius Lab	GERMANY
2	Hotplate stirrer	LabTech	KOREA
3	DSC (Differential Scanning Calorimeter) Thermal Analyzer	Shimadzu	JAPAN
4	1-stage vacuum pump 5 Pa ¼ HP	Wenling Aitcool	CHINA
5	Melting point apparatus	BioCote	UK
6	CHN Elemental Analyzer	EURO EA 3000	ITALY
7	Clean Bench	LabTech	KOREA
8	Incubator UN 55	Memmert	GERMANY
9	Microplate reader 800 TS	BioTek	USA
10	Inverted Microscope	Zeiss	GERMANY

3

### **Table 3**(on next page)

Select chemical parameters of the spebrutinib standard and the synthesized compounds.

1 Table (4) Select chemical parameters of the spebrutinib standard and the synthesized compounds.

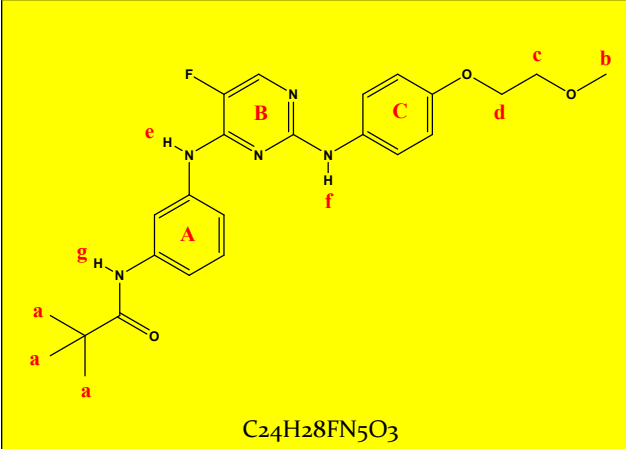
Compound symbol	Molecular mass	Yield %	H Bond Donor Count	H Bond Acceptor Count	Rotatable bond count	Heavy atom count
AVL-292	423.45	STD	3	8	10	27
2a	473.51	89	3	8	10	35
2b	453.52	86	3	8	14	33

2

# **Table 4**(on next page)

1H NMR data and the interpretations of compound 2b.

1 Table (7) <sup>1</sup>H NMR data and the interpretations of compound 2b.

 $C_{24}H_{28}FN_5O_3$				
Chemical group	Chemical Shift (ppm)	Integrations	No. of Hydrogens	Interpretations
a	1.16	8.94	9	Singlet, for CH <sub>3</sub> protons
b	3.32	3.15	3	Singlet, for CH <sub>3</sub> protons
c	3.65	2.13	2	Triplet, for CH <sub>2</sub> protons
d	4.03	2.03	2	Triplet, for CH <sub>2</sub> protons
A+B+C	6.63-8.09	9.57	9	Aromatics, rings; A, B, C, and D.
e	9.03	0.96	1	Singlet, for N-H proton as indicated.
f	9.21	0.99	1	Singlet, for N-H proton as indicated.
g	9.36	0.67	1	Singlet, for N-H proton as indicated.
		Sum= 28.44	Total= 28	



# **Table 5**(on next page)

Elemental microanalyses of spebrutinib and the synthesized compounds.

1

2 Table (5) Elemental microanalyses of spebrutinib and the synthesized compounds.

Compound symbol	Chemical formula	Molecular mass	Elemental microanalyses %		
			Element	Calculated	Observed
AVL-292	C <sub>22</sub> H <sub>22</sub> FN <sub>5</sub> O <sub>3</sub>	423.45	C	62.400	62.358
			H	5.240	5.191
			N	16.540	16.452
			Sum	84.18	84.001
			% Deviation	0.21%	
2a	C <sub>26</sub> H <sub>24</sub> FN <sub>5</sub> O <sub>3</sub>	473.51	C	65.950	65.897
			H	5.110	4.920
			N	14.790	14.718
			Sum	85.85	85.535
			% Deviation	0.37%	
2b	C <sub>24</sub> H <sub>28</sub> FN <sub>5</sub> O <sub>3</sub>	453.52	C	63.560	63.470
			H	6.220	6.195
			N	15.440	15.293
			Sum	85.22	84.958
			% Deviation	0.31%	

3

## Table 6 (on next page)

Some of the physical parameters of spebrutinib and the synthesized analogues.

\*tPSA = topological polar surface area.

\*\* melting points were observed with DSC.

1 Table (3) Some of the physical parameters of spebrutinib and the synthesized analogues.

Compound symbol	Physical appearance	m.p. (°C)**	Log P	tPSA*
AVL-292	White powder	174.68	3.72	96.34 A <sup>2</sup>
2a	Faint yellowish-brown crystals	148.92	4.94	96.34 A <sup>2</sup>
2b	White fluffy powder	152.06	4.97	96.34 A <sup>2</sup>

2 \*tPSA = topological polar surface area.

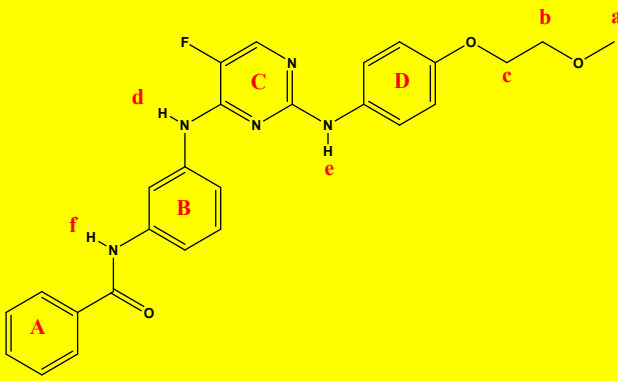
3 \*\* melting points were observed with DSC.

# **Table 7** (on next page)

<sup>1</sup>H NMR data and the interpretations of compound 2a.

1

2 Table (6) <sup>1</sup>H NMR data and the interpretations of compound 2a.

 <p style="text-align: center;">C<sub>26</sub>H<sub>24</sub>FN<sub>5</sub>O<sub>3</sub></p>				
Chemical group	Chemical Shift (ppm)	Integrations	No. of Hydrogens	Interpretations
a	3.32	3.00	3	Singlet, for CH <sub>3</sub> protons
b	3.65	1.80	2	Triplet, for CH <sub>2</sub> protons
c	4.04	1.94	2	Triplet, for CH <sub>2</sub> protons
A+B+C+D	6.38-7.66	14.43	14	Aromatics, rings; A, B, C, and D.
d	8.06	1.01	1	Singlet, for N-H proton as indicated.
e	8.96	0.98	1	Singlet, for N-H proton as indicated.
f	9.07	0.98	1	Singlet, for N-H proton as indicated.
		Sum= 24.14	Total= 24	

3

# **Table 8**(on next page)

A summary for IC50 for the cell lines and chemical compounds specified.

1

2 **Table (8) a summary for IC<sub>50</sub> for the cell lines and chemical compounds specified.**

Cell line	IC <sub>50</sub> AVL-292	IC <sub>50</sub> 2a	IC <sub>50</sub> 2b
HCT116	11.73 µg/mL	34.05 µg/mL	25.53 µg/mL
MCF-7	13.566 µg/mL	10.744 µg/mL	19.23 µg/mL
MDCK	4.011 mg/mL	8.653 mg/mL	1.705 mg/mL

3

# Figure 1(on next page)

the percent viable cells versus concentration of compound 2a after 24-hours' incubation of HCT116 colorectal cancer cell line.

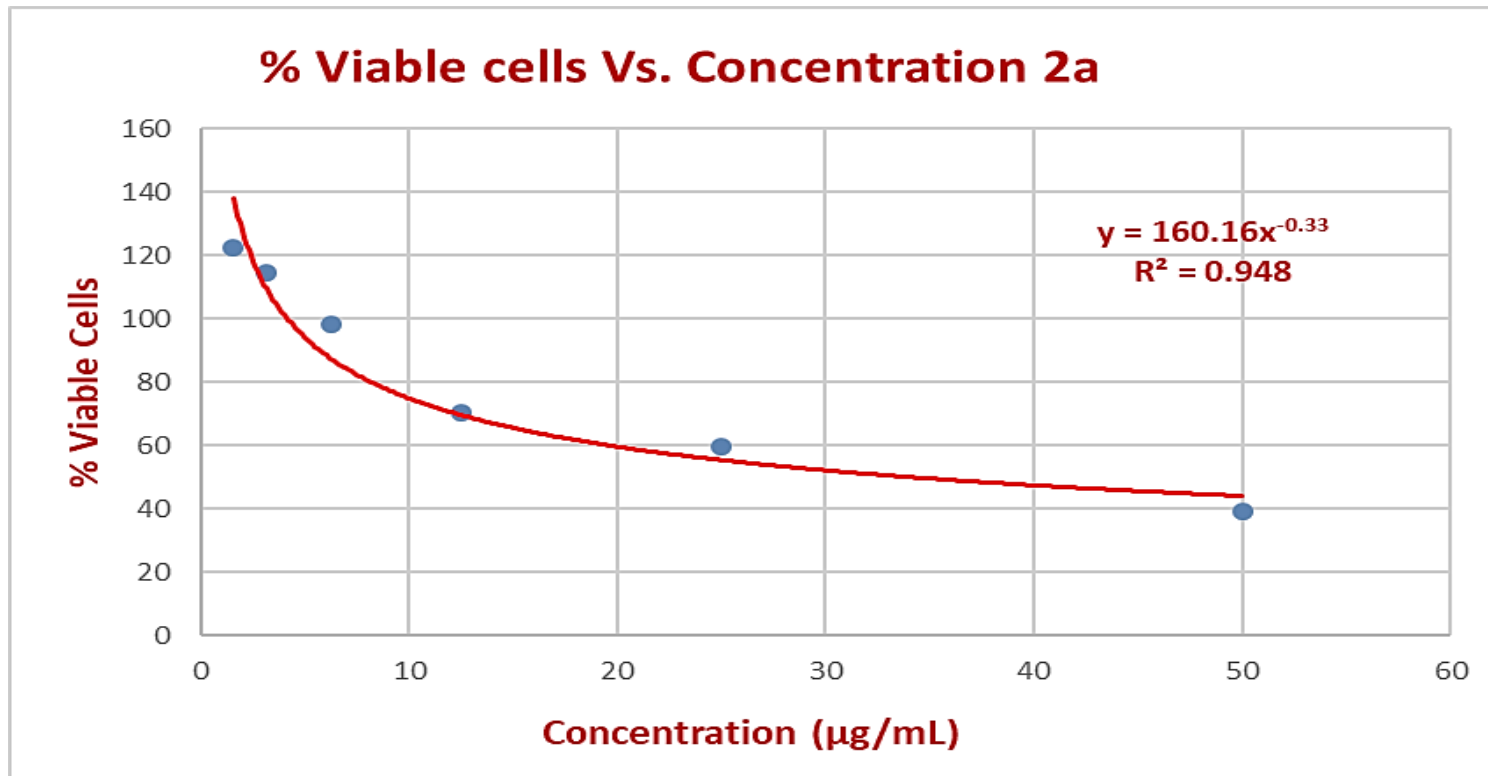


Figure (2) the percent viable cells versus concentration of compound 2a after 24-hours' incubation of HCT116 colorectal cancer cell line.

## Figure 2 (on next page)

the percent viable cells versus concentration of spebrutinib standard after 24-hours' incubation of MCF-7 breast cancer cell line.

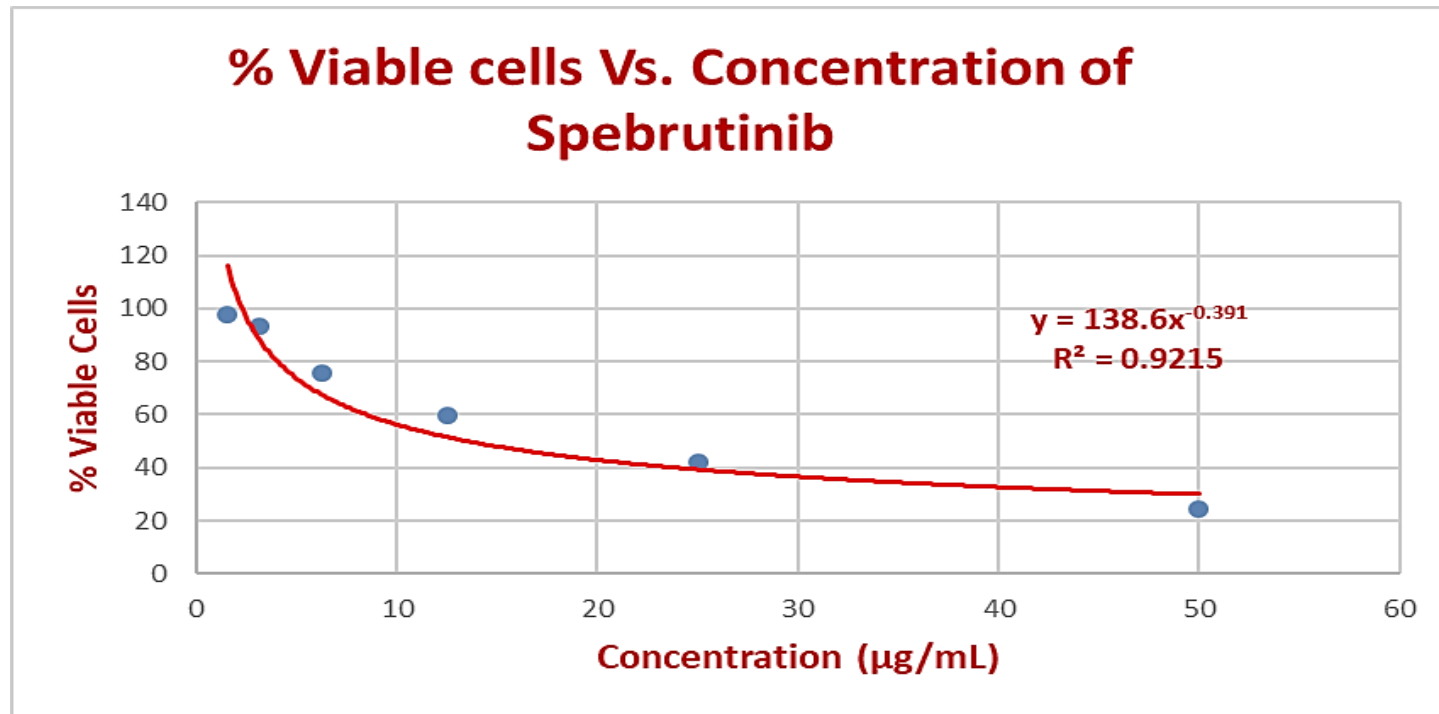


Figure (4) the percent viable cells versus concentration of spebrutinib standard after 24-hours' incubation of MCF-7 breast cancer cell line.

# Figure 3(on next page)

the percent viable cells versus concentration of compound 2b after 24-hours' incubation of MCF-7 breast cancer cell line.

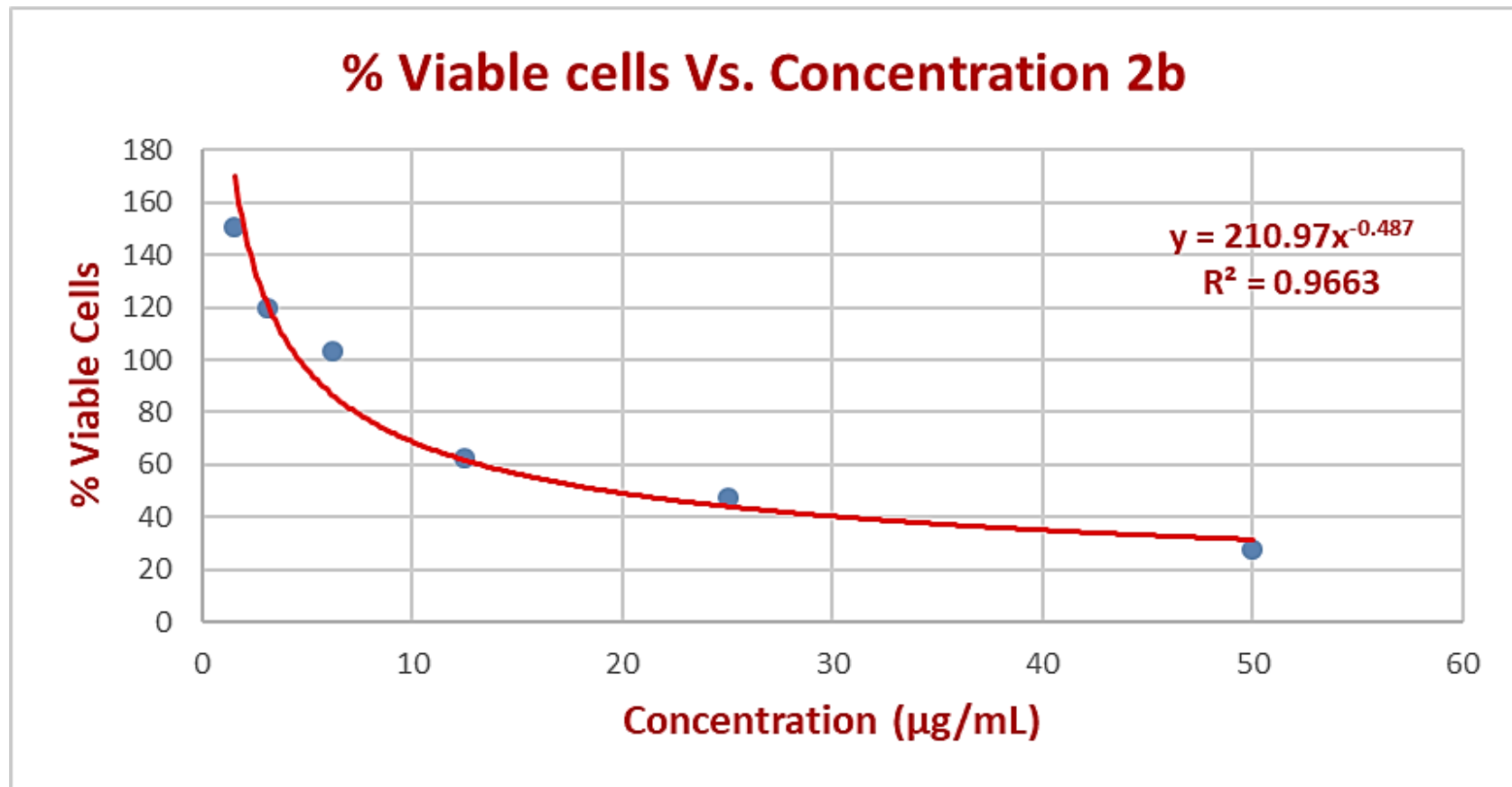


Figure (6) the percent viable cells versus concentration of compound 2b after 24-hours' incubation of MCF-7 breast cancer cell line.

# Figure 4 (on next page)

the percent viable cells versus concentration of compound 2a after 24-hours' incubation of MCF-7 breast cancer cell line.

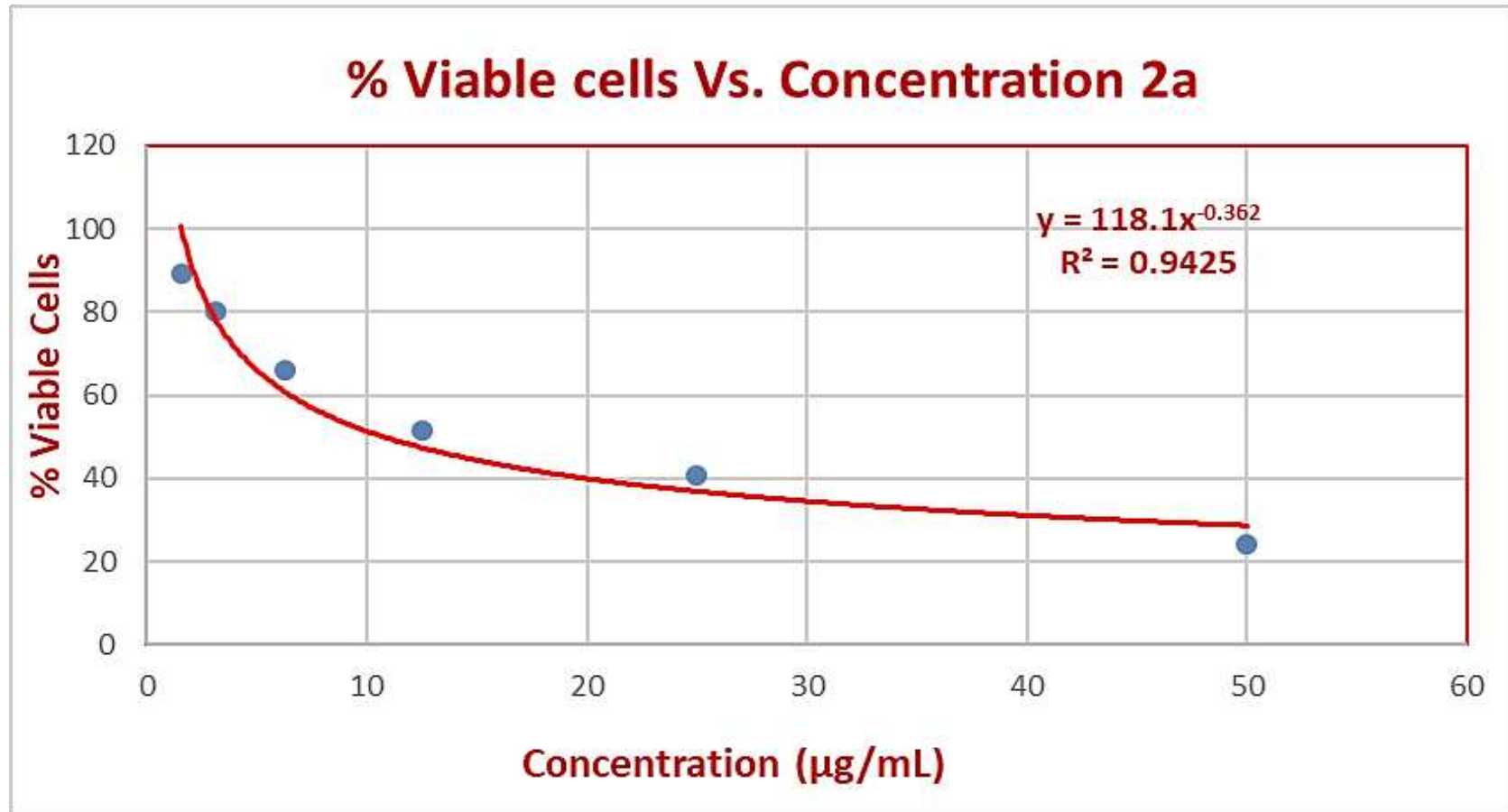


Figure (5) the percent viable cells versus concentration of compound 2a after 24-hours' incubation of MCF-7 breast cancer cell line.

# Figure 5(on next page)

the percent viable cells versus concentration of spebrutinib standard after 24-hours' incubation of MDCK kidney normal cell line.

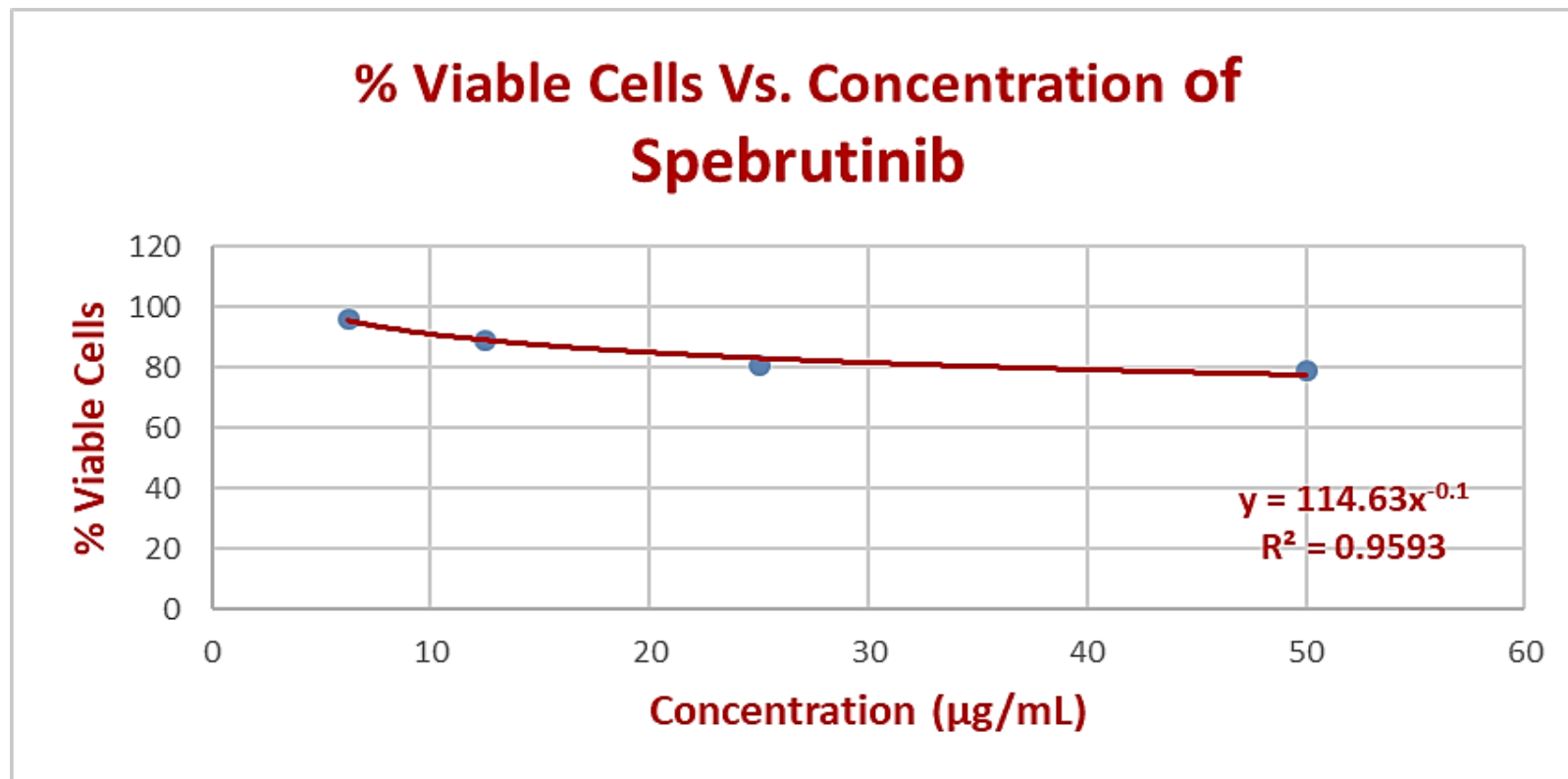


Figure (7) the percent viable cells versus concentration of spebrutinib standard after 24-hours' incubation of MDCK kidney normal cell line.

# Figure 6 (on next page)

the percent viable cells versus concentration of compound 2a after 24-hours' incubation of MDCK kidney normal cell line.

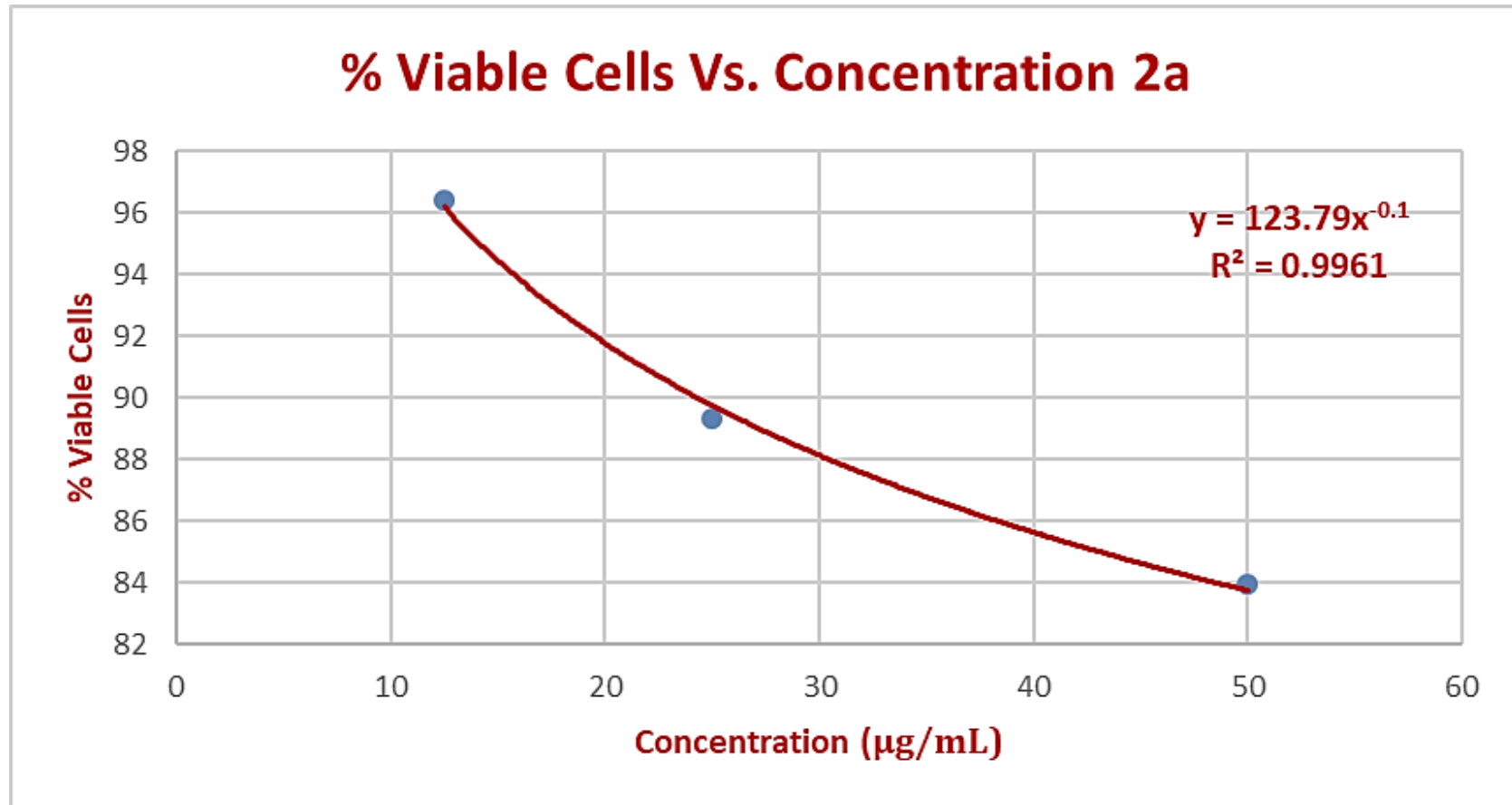


Figure (8) the percent viable cells versus concentration of compound 2a after 24-hours' incubation of MDCK kidney normal cell line.

# Figure 7 (on next page)

the percent viable cells versus concentration of spebrutinib standard after 24-hours incubation of HCT116 colorectal cancer cell line.

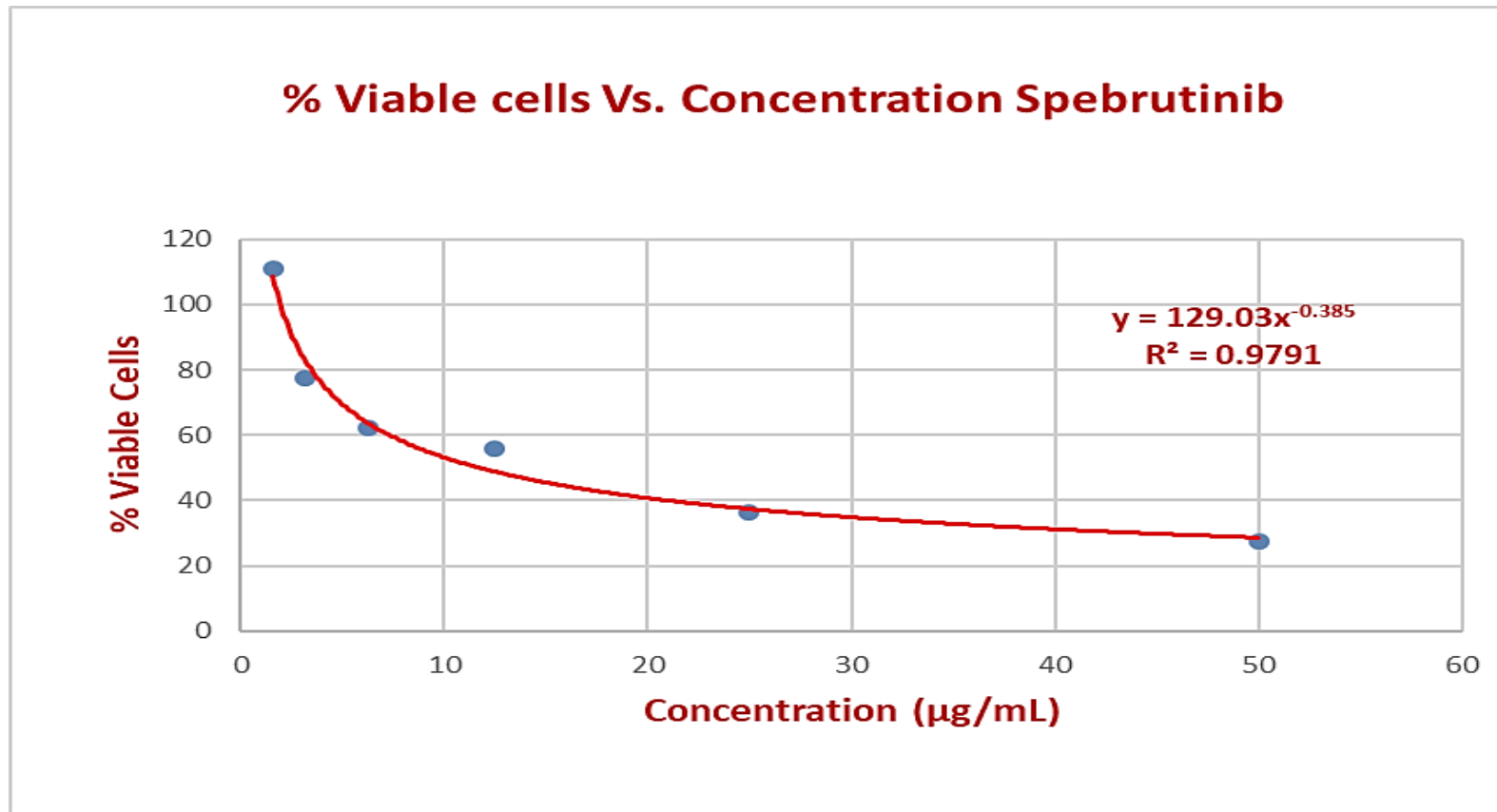


Figure (1) the percent viable cells versus concentration of spebrutinib standard after 24-hours' incubation of HCT116 colorectal cancer cell line.

# Figure 8 (on next page)

the percent viable cells versus concentration of compound 2b after 24-hours incubation of MDCK kidney normal cell line.

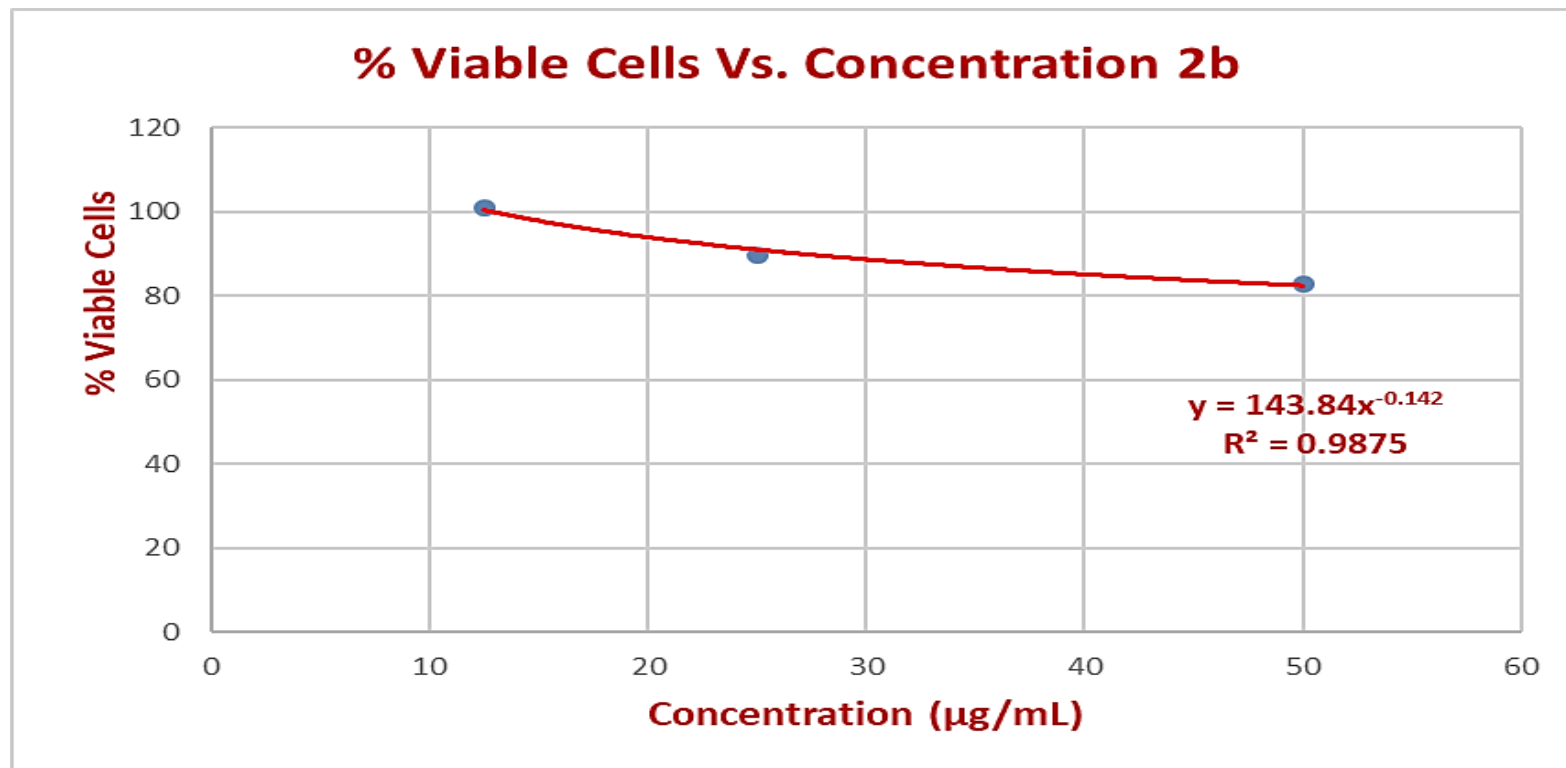


Figure (9) the percent viable cells versus concentration of compound 2b after 24-hours' incubation of MDCK kidney normal cell line.

# Figure 9 (on next page)

the percent viable cells versus concentration of compound 2a after 24-hours incubation of HCT116 colorectal cancer cell line.

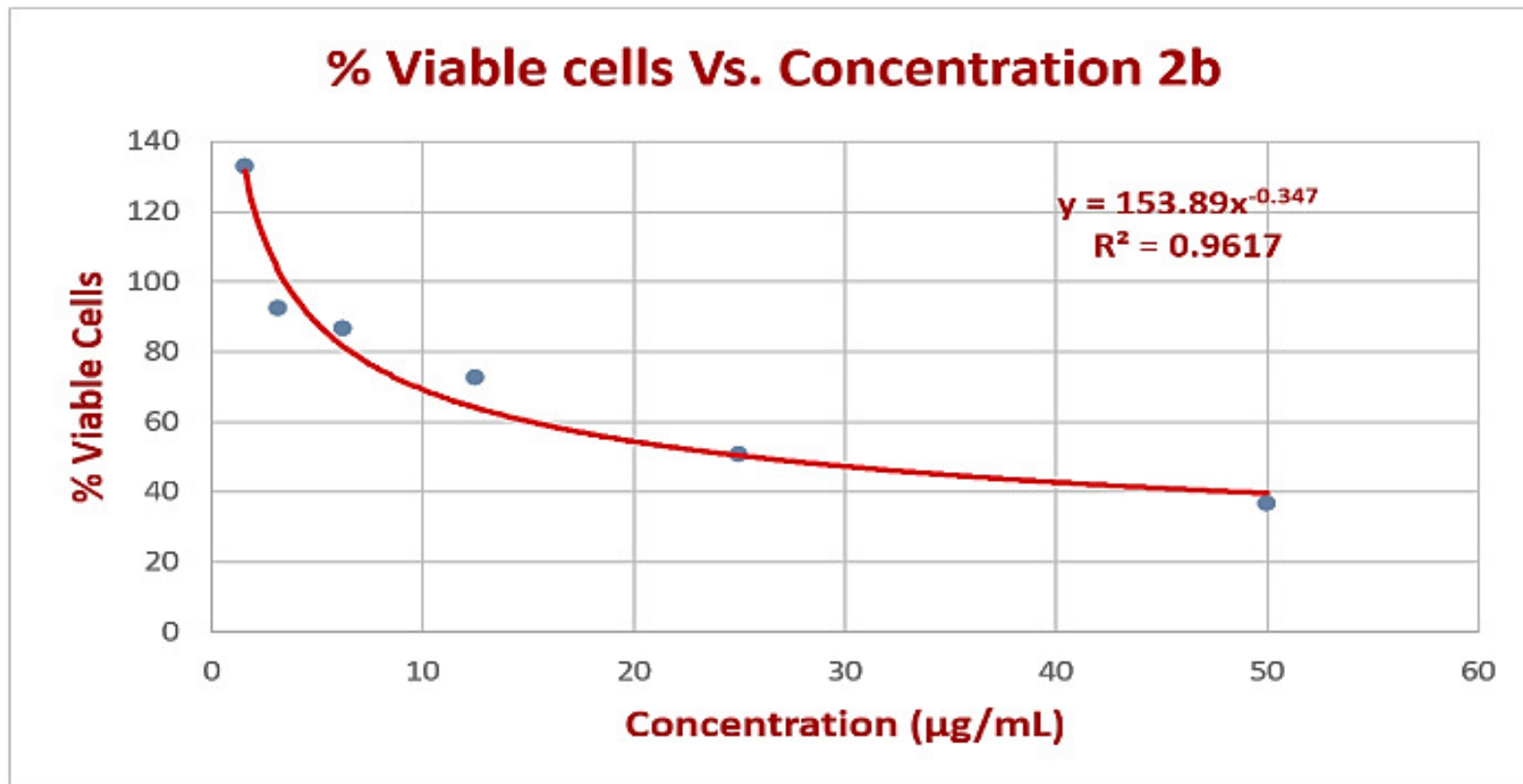
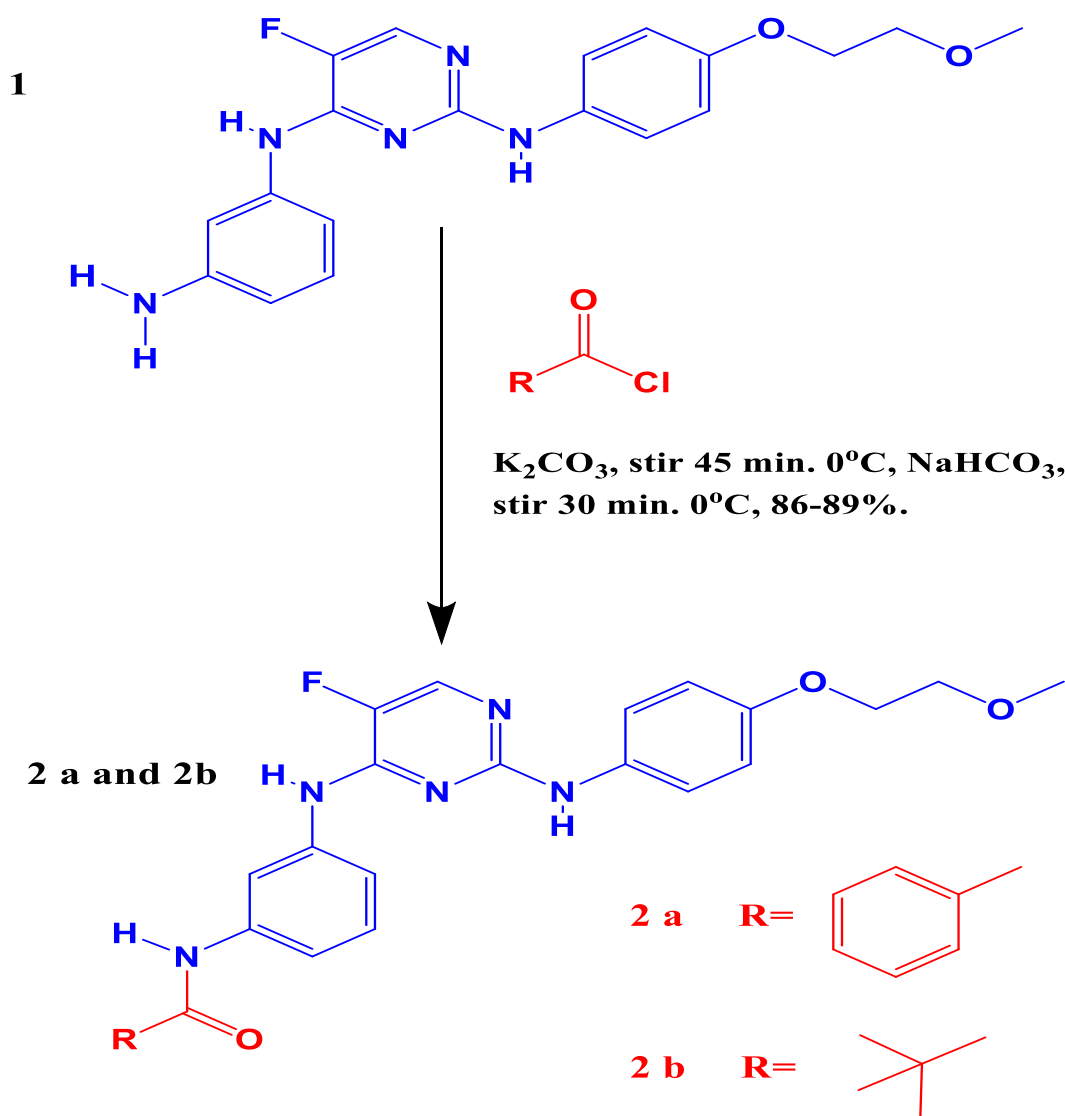


Figure (3) the percent viable cells versus concentration of compound 2a after 24-hours' incubation of HCT116 colorectal cancer cell line.

# **Figure 10**(on next page)

reveals the chemical syntheses and reaction conditions of compounds 2a and 2b.



Scheme (1) reveals the chemical syntheses and reaction conditions of compounds 2a and 2b.